

Manifestations of Magnetic Field Inhomogeneities

Lawrence Rudnick

University of Minnesota, Minneapolis, MN 55455, USA

e-mail: larry@astro.umn.edu

Abstract. Both observations and simulations reveal large inhomogeneities in magnetic field distributions in diffuse plasmas. Incorporating these inhomogeneities into various calculations can significantly change the inferred physical conditions. In extragalactic sources, e.g., these can compromise analyses of spectral ageing, which I will illustrate with some current work on cluster relics. I also briefly re-examine the old issue of how inhomogeneous fields affect particle lifetimes; perhaps not surprisingly, the next generation of radio telescopes are unlikely to find many sources that can extend their lifetimes from putting relativistic electrons into a low-field ‘freezer’. Finally, I preview some new EVLA results on the complex relic in Abell 2256, with implications for the interspersing of its relativistic and thermal plasmas.

Key words. Radiation mechanisms: nonthermal—galaxies: clusters—magnetic fields.

1. Introduction

Simulations of magnetic fields in radio galaxies and clusters of galaxies show quite filamentary structures, generated by turbulent-like motions. Figure 1 shows a

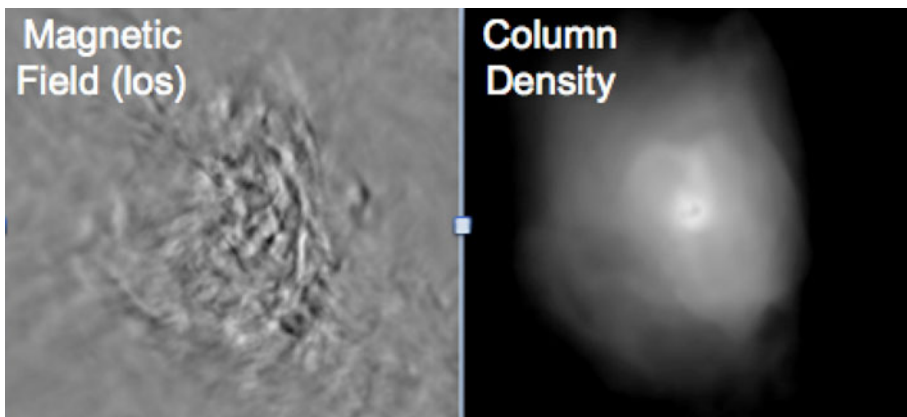


Figure 1. 3 Mpc field encompassing a relaxed cluster; extracted from MHD cosmological simulation by K. Dolag under analysis by A. Johnson, P. Mendygral and T. W. Jones.

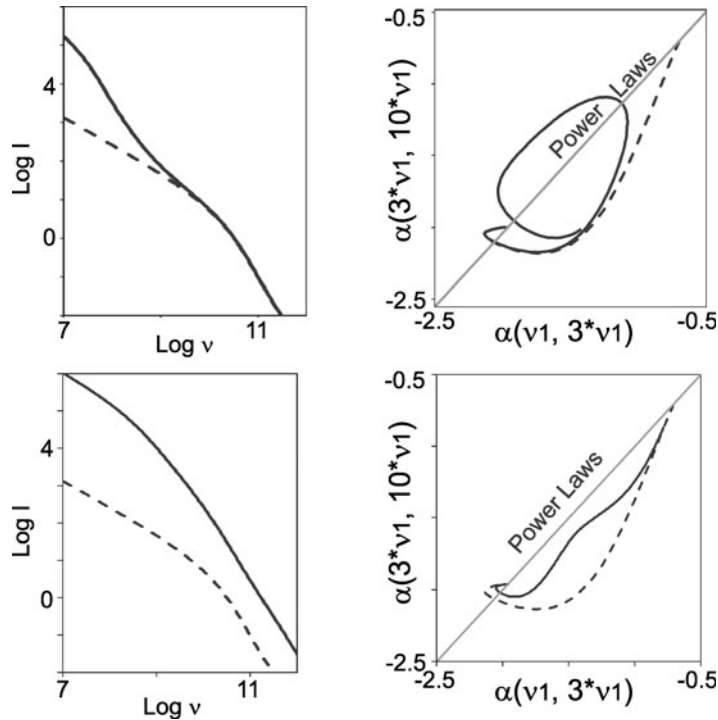


Figure 2. Spectra and color–color diagrams for a two-component model (*top*) and for a power-law magnetic field distribution (*bottom*). Dashed lines – single component.

comparison between the magnetic field and density distributions in a *relaxed* cluster selected from a cosmological simulation. Even in this case, the magnetic field shows considerably more fine-scale structures; this changes how we interpret observations.

The new generation of radio telescopes such as the EVLA, LOFAR, and the SKA precursors will provide the tools to examine these inhomogeneities for extragalactic sources, similar to what already occurs in galactic studies. The following discussion is largely from the perspective of the physical properties of galaxy cluster sources – halos and peripheral relics (gischt, Kempner *et al.* 2004), although the implications are more general.

We can characterize the magnetic field structure at four different levels:

- *Average or rms field strength*, estimated e.g., by minimum energy arguments, occasionally through joint radio/X-ray inverse Compton analyses.
- *Rms fluctuations*, from brightness and/or polarization variations.
- *Fluctuation power on various scales*, using the power spectrum or structure function. These are often based, for clusters, on the rotation measure distribution of cluster sources (e.g., Bonafede *et al.* 2010). This procedure has serious flaws unless it accounts for contributions local to the source (Rudnick and Blundell 2003; Laing *et al.* 2008).
- *Topology of the magnetic field*, which can vary greatly while leaving the all of the above measures unchanged (Waelkens *et al.* 2009).

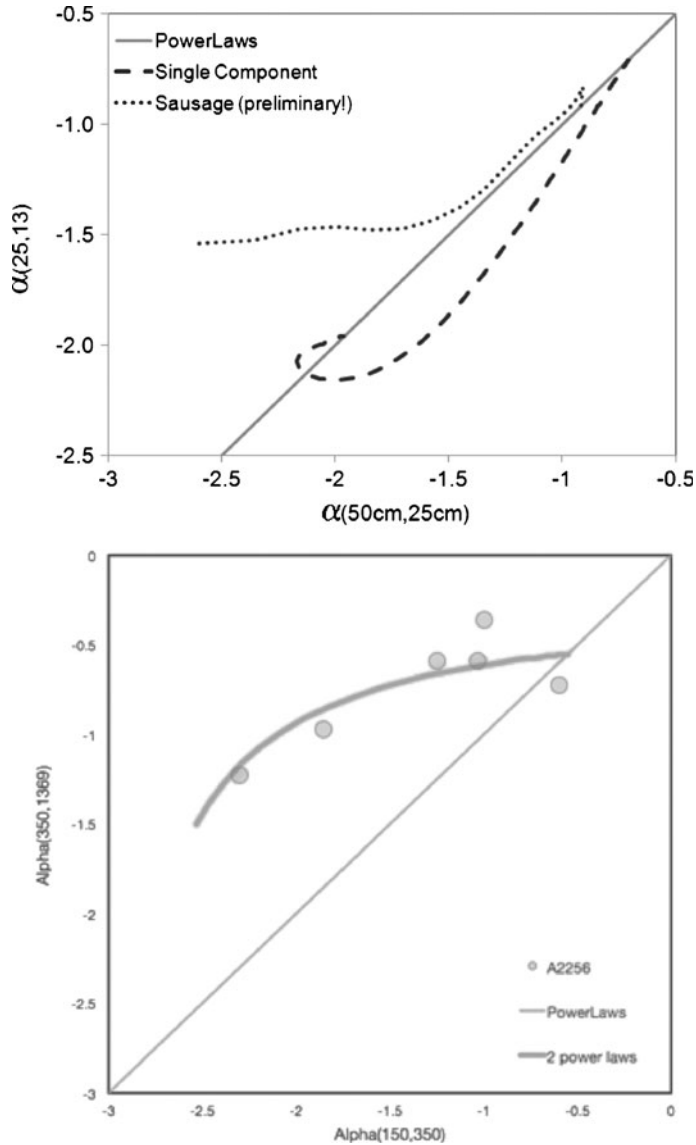


Figure 3. *Top:* C–C diagram of sausage relic (van Weeren *et al.* 2010) – data, dotted line; homogeneous spectrum – dashed; *Bottom:* C–C for Abell 2256 – data from Ruta and Dwarakanath (2010) with a two-component model.

Here, I look just at the effect of fluctuations, without regard for scale or topology.

2. Spectral shapes and radiative ages

Extragalactic astronomers use gradients in spectral index as indicators of the relativistic electron radiative losses. Coupled with a model for the field, these are then

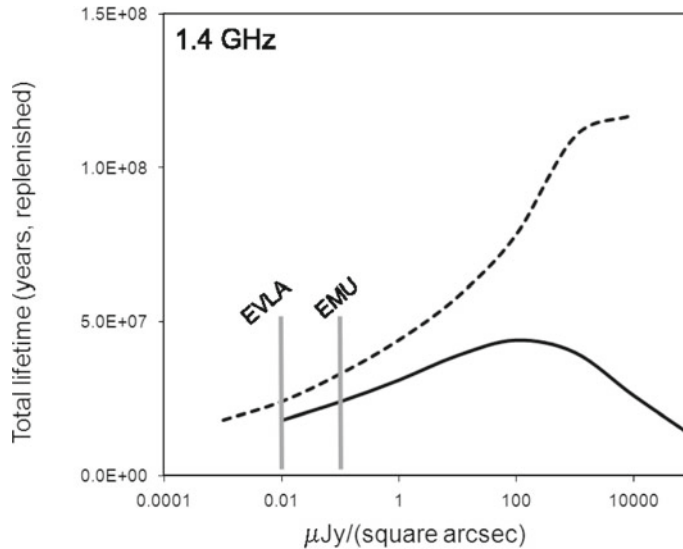


Figure 4. Electron lifetimes against all losses as a function of surface brightness. Solid line – homogeneous field; Dashed line – 10% filling factor. Characteristic EMU and EVLA sensitivity limits are shown.

used to calculate ages since the particles were accelerated and thus flow speeds from the acceleration site. Figure 2 illustrates how spectral shapes change in inhomogeneous fields, even with the same distribution of relativistic electrons. The simplest example is two different magnetic fields within one observing beam. This changes the spectral shape, and its corresponding color–color diagram (Katz-Stone *et al.* 1993); in particular the spectrum can be concave instead of the standard convex shape for radiative losses. Any points in the upper left of the color–color diagram represent a concave portion of the spectrum.

A second simple example is the power law distribution of magnetic fields, again with a fixed electron population. In this case, the spectrum broadens, and tends to approach the power-law line in the color–color diagram. That is, the spectrum may appear to be a power-law around each frequency, but that power law slowly changes as a function of frequency.

Analysis of these simple inhomogeneous cases leads to the following insights:

- Changes in spectrum from one place to the next do *not* necessarily imply ageing; they can arise simply from changing the combination of magnetic fields.
- The observation of a power-law does *not* necessarily reflect the initial electron spectrum, and therefore cannot be used to derive, e.g., shock Mach numbers.

It is therefore essential to analyse the spectral *shape* before inferring the physics. Standard spectral analyses of Abell 2256 and CIZA J2242.8+5301 have been cited as support for the acceleration of particles at the leading edge of outward moving shocks from cluster mergers (peripheral relics), followed by radiative ageing (Clarke and Enßlin 2006; van Weeren *et al.* 2010). Figure 3, by contrast, shows that the

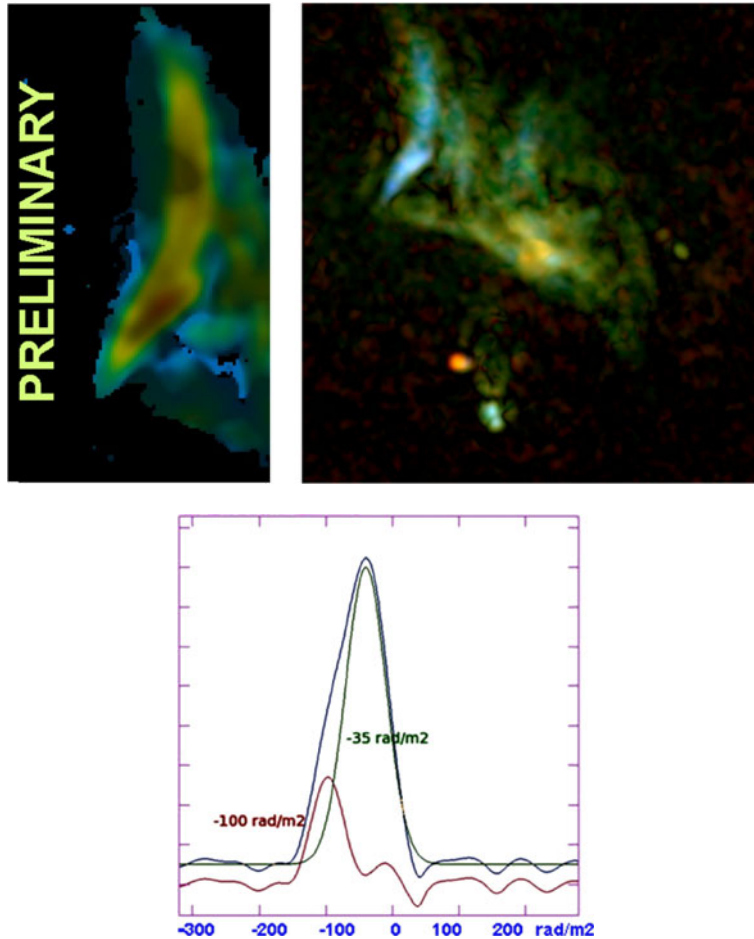


Figure 5. Preliminary EVLA 1–2 GHz observations of Abell 2256 RMs. Color: peak RM at each location (different scales: *left* and *right*); Brightness: polarized intensity. *Bottom*: Preliminary example of a Faraday spectrum (intensity as a function of rotation measure) from the relic of Abell 2256; a gaussian component at -35 rad/m^2 is subtracted, leaving residual emission at -100 rad/m^2 .

spectral shapes in these cases are more complex than assumed, and ageing of a homogeneous electron population is not appropriate. In the case of Abell 2256, there are likely two dominant components, one from the relic and one from the (underlying) steeper spectrum halo, as also suggested by Ruta and Dwarakanath (2010). In the case of the ‘sausage’ relic, a more complicated post-shock magnetic field behavior, and a possible additional diffuse component, are likely necessary¹.

¹Work in progress with R. van Weeren, H. Röttgering, M. Brüggen and M. Hoeft.

3. The ‘freezer’

In cluster halos and many radio galaxies, there appears to be a need to accelerate relativistic particles *in situ*, i.e., throughout the plasma, instead of at a single site. This arises from short radiative loss times, which are dominated by synchrotron and inverse Compton radiation (see full summary of losses in Sarazin (1999)). One idea, originated by S. Spangler as the ‘sewer rat model’, is to extend the electron lifetimes by putting them into a low-field ‘freezer’ where their lifetimes are limited by inverse Compton scattering off the CMB. Then, at a fixed observing frequency, the high-field regions produce radiation from lower energy electrons, gaining an even further advantage over a homogeneous field of the same average value. Figure 4 shows the resulting lifetimes for sources of fixed surface brightnesses, assuming that the minimum energy derived field is approximately correct. Filling factors for high-field regions of 100% and 10% are used, with a field strength of zero in the low field regions (a very extreme case). We can see that as one approaches the low surface brightnesses achievable with the next generation telescopes, and discovers new sources, there is little gain in the electron lifetime from a zero-field freezer.

4. Mixing thermal and relativistic plasmas

Figure 5 shows some very preliminary results on rotation measures (RM) in the Abell 2256 peripheral relic² using the new EVLA 1–2 GHz system. The exquisite sensitivity and broad coverage in λ^2 space allows us to measure subtle variations in RMs across the relic. The two color figures show variations of ≈ 10 rad/m² across the relic; different filaments can be seen to have different RMs, so the RM structure (thermal) is related to the synchrotron emitting structure. Rather than a foreground RM screen, we are thus seeing inside the first 3D thermal/relativistic distribution. Figure 5, right, is an RM synthesis spectrum, showing that multiple RMs can sometimes be seen along the same line-of-sight. Multiple RM components have also been recently seen in Abell 2255 radio galaxies (Pizzo *et al.* 2011). We are thus on the threshold of looking at how thermal and relativistic plasmas mix and interact with each other, mediated by shocks and turbulence.

Acknowledgements

This work is supported, in part, by U.S. National Science Foundation grant AST-0908688 to the University of Minnesota. The National Radio Astronomy Observatory/EVLA is operated by Assoc. Univ. Inc. under co-operative agreement with the U.S. National Science Foundation.

References

- Bonafede, A. *et al.* 2010, *Astron. Astrophys.*, **513**, 30.
 Clarke, T., Enßlin, T. 2006, *Astron. J.* **131**, 2900.
 Katz-Stone, D., Rudnick, L., Anderson, M. 1993, *Ap. J.*, **407**, 549.

²F. Owen, P. I., with J. Eilek, U. Venkata Rao, S. Bhatnagar, L. Kogan, and L. Rudnick.

- Kemper, J. *et al.* 2004, in Reiprich, T., Kempner, J. & Soker, N., editors, *The Riddle of Cooling Flows in Galaxies and Clusters of Galaxies*, <http://www.astro.virginia.edu/coolflow>.
- Laing, A., Bridle, A. H., Parma, P., Murgia, M. 2008, *Mon. Not. R. Astron. Soc.*, **391**, 521.
- Pizzo, R. *et al.* 2011, *Astron. Astrophys.* **525**, 104.
- Rudnick, L., Blundell, K. M. 2003, *Ap. J.*, **588**, 143.
- Ruta, K., Dwarakanath, K. 2010, astro-ph:1005.3604.
- Sarazin, C. 1999, *Ap. J.*, **520**, 529.
- van Weeren, R., Röttgering, H., Brügger, M., Hoeft, M. 2010, *Nature*, **330**, 347.
- Waelkens, A., Schekochihin, A., Enßlin, T. 2009 *Mon. Not. R. Astron. Soc.*, **398**, 1970.